

Comparison of Homopolar and Heteropolar Bearingless Reluctance Slice Motor Prototypes

Wolfgang Gruber^a, Walter Bauer^a, Karlo Radman^b

^a Johannes Kepler University Linz, Altenberger Str. 69, 4040 Linz, Austria, wolfgang.gruber@jku.at

^b University of Rijeka, Faculty of Engineering, Vukovarska 58, 51000 Rijeka, Croatia

Abstract—This paper focuses on the operational behavior of two bearingless reluctance slice motor prototypes. After a brief introduction of the two systems, experiences, obtained from both novel bearingless drives, are presented. On this basis, communalities and differences, in various areas, e.g. construction, geometric constraints, winding systems, force to torque ratio, power electronic utilization and efficiency, will be outlined. This will help to point out the applicability of the reluctance slice motor concepts for industrial utilization.

I. INTRODUCTION

A. Bearingless Reluctance Slice Motors

Contactless operation and therefore, no lubrication, no mechanical wear and loss, extreme cleanness and purity, superior tightness as well as no need for seals are advantages of magnetically levitated systems. However, due to the relatively high cost magnetic levitation is normally used in very specialized areas and has not been implemented in large scale mass production. A design that has the capability to reduce the mechanical complexity and therefore production cost, are bearingless motors. These magnetically levitated drives are very compact and combine the generation of motor torque and suspension force in one common unit. The passive stabilization of various degrees of freedom by a permanent magnetic flux in the air gap further reduces the complexity. In bearingless slice motors the axial and tilting directions are passively stabilized and the radial suspension forces and the motor torque are created actively, featuring a fully magnetically levitated system of low mechanical complexity [1]. Pumps [2] and stirrers [3] are the main field of application for this topology by now.

However, the passive air gap field is normally created by permanent magnets located in the rotor. Thus, the rotor of bearingless motors resembles rotors of synchronous machines, with surface mounted, interior or inset permanent magnets [4]. Only recently, first theoretical works have been published on bearingless slice motors that have no permanent magnets in the rotor, but in the stator. These designs are called bearingless reluctance slice motors. No permanent magnets lead to very cheap and robust rotors. This is important especially in disposables and high temperature applications. In previous works the authors introduced theoretical considerations about homopolar and heteropolar bearingless reluctance slice motors [5]. Homopolar drives feature a unipolar permanent magnetic field in the air gap, whereas heteropolar drives possess

alternating permanent magnetic air gap field. Based on that work, two prototype drives have been optimized, fabricated and put into operation recently [6], [8]. This paper now focuses on the experiences obtained from the manufactured heteropolar and homopolar bearingless motor and points out the differences in their characteristic behaviour based on measurement results.

B. Homopolar Design

The setup of the homopolar bearingless reluctance slice motor is depicted in Fig. 1. The rotor is an iron ring featuring four salient poles on the outer side and a circular surface on the inside. The stator composition resembles a temple motor design [1], where the six stator teeth are bent in axial direction and are closed over a back yoke plate on the bottom of the system. Hence, the winding axes of the stator coils are parallel to the rotor axis. However, common temple motor designs do not have a stator permanent magnet and the stator flux collector plate. It is also visible that the illustrated design features two radial air gaps between rotor and stator. There is one gap between the stator teeth and the rotor and an additional one between the rotor and the stator flux collector plate. The cylindrical stator permanent magnet is axially magnetized and creates a homopolar bias flux in both air gaps. The electromagnetic flux created by the stator coils passes

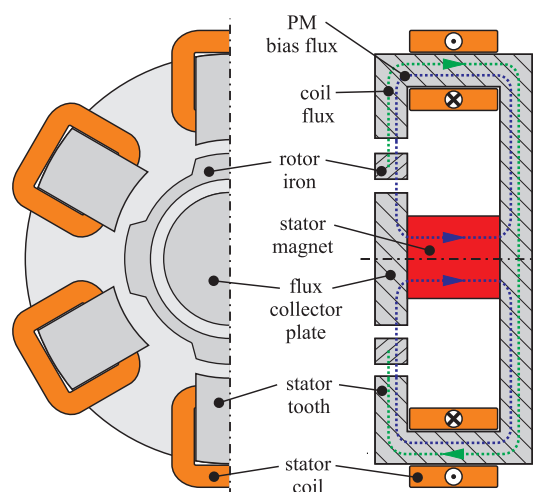


Figure 1. Composition of an 6/4 bearingless homopolar reluctance slice motor (featuring six stator teeth and four rotor teeth).

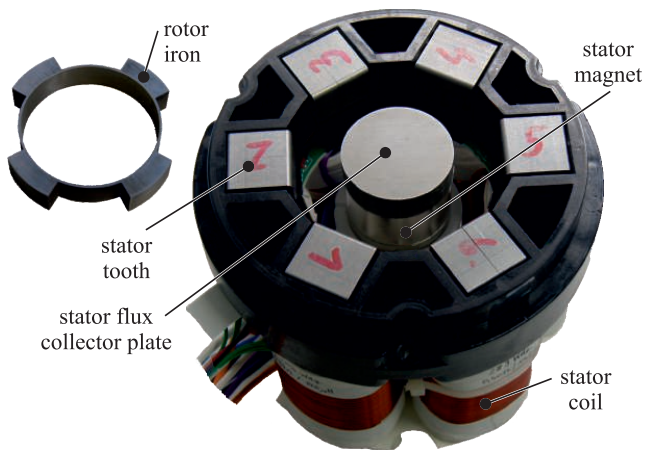


Figure 2. Rotor and stator of the bearingless homopolar reluctance slice motor prototype.

over the stator teeth and the rotor. Thus, the flux collector plate and the stator permanent magnet are not permeated by the coil flux path. However, each one of the six stator coils is capable to create coupled radial bearing forces and drive torque in dependence on the rotor angle.

Figure 2 depicts a photo of the manufactured prototype [6]. The six concentric coils are connected in two double star systems. All phases are capable to create both radial suspension forces and motor torque in dependence on the rotor angle.

C. Heteropolar Design

The main and striking constructional characteristic of the flux-switching motor, depicted in Fig. 3 and 4, is the placement of the permanent magnets. They are located in the midst of the stator teeth and separate them electromagnetically. The flux lines of each permanent magnet close mainly over the neighbouring stator teeth and, thus, do not penetrate the whole air gap, but only influence the air gap region close to the permanent magnet, creating two opposing magnetic poles in the air gap and therefore a heteropolar magnetic air gap field around the circumference. Unfortunately, there is also a considerable amount of fringing flux closing over the outer side of the stator. To keep this kind of stray flux low, a small air gap length (compared to the magnet width) is favourable and necessary.

However, the air gap flux density in flux-switching machines is often higher than in comparable other electric machines, leading to an increased torque capacity [9]. This is due to the flux concentration capability of the construction. The surfaces of the stator teeth normal to the magnetization direction collect permanent magnetic flux and concentrate it towards the much smaller area of the stator teeth adjoining the air gap.

In this novel kind of bearingless motor, two separated three phase winding systems are placed. One phase consists of two opposing coils. In dependence of their referring coil turn direction, either suspension force or drive torque is created by the considered phase. Thus, in contrast to the con-

sidered homopolar reluctance drive, radial suspension force and torque generation are decoupled in this bearingless drive.

The prototype features twelve stator coils and a rotor with ten poles [8]. Figure 4 depicts a picture of the manufactured bearingless flux-switching motor. The stator iron is held in an aluminium frame to strengthen the structure. The permanent magnets are glued in pockets that separate the stator elements. The externally wound stator coils are easily slipped on the stator teeth and connected accordingly.

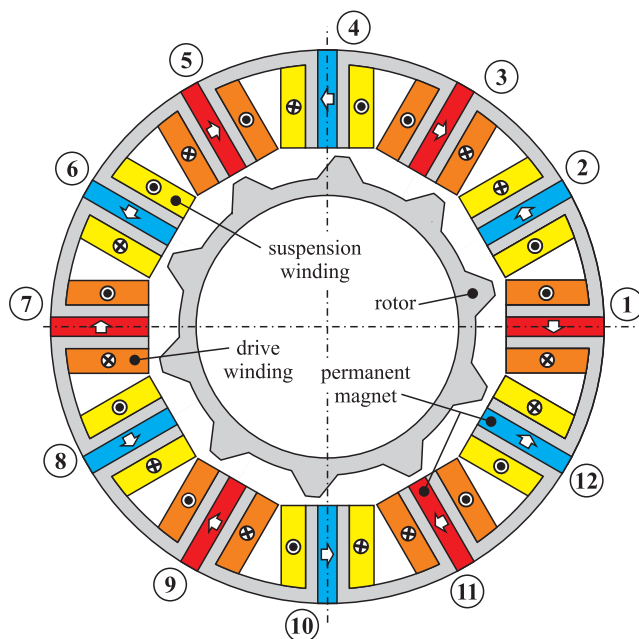


Figure 3. Principle cross section of the built flux-switching motor with twelve stator and ten rotor teeth. The arrows indicate the direction of the magnetization.

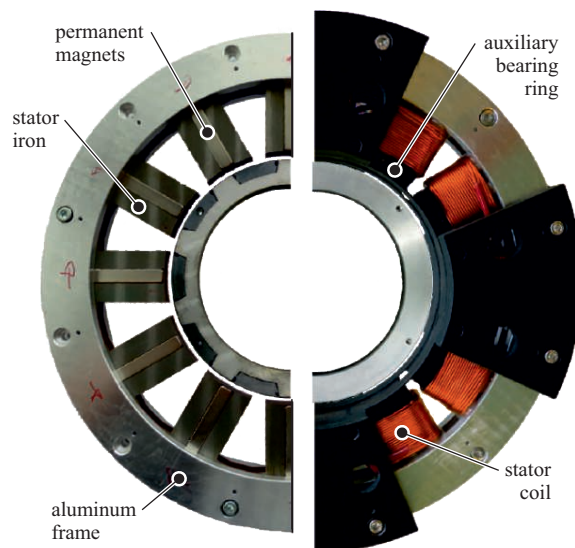


Figure 4. Stator of the bearingless flux-switching slice motor prototype without coils (left) and fully assembled (right).

II. COMPARISON OF THE SYSTEMS

Both systems feature very different geometric sizes but are driven by the same power electronics, featuring six half bridges with a DC voltage link of 300V and a maximum effective current of 15A. Thus, the electrical maximum input power is the same. In the following sections certain characteristics of the two prototypes are considered and discussed.

A. Geometric System Values

The two considered bearingless reluctance slice motor prototypes feature a quite different geometry. Table I summarizes the main values. Comparing the gap factor

$$g = \frac{\delta}{d_{ro}} \quad (1)$$

with $g_{hom} = 0.074$ and $g_{het} = 0.02$ it becomes obvious that the heteropolar flux-switching motor seems not very suitable for large air gaps. This originates from the distinct permanent magnetic fringing flux paths (on the outer side of the stator), that rise significantly with increasing air gap. Thus, the performance of the flux-switching designs decreases strongly for larger air gaps. This is not the case for the homopolar design.

B. Force and Torque Generation

The generation of force and torque works very different in the two considered systems. As indicated in [6] for the homopolar motor, each single phase creates both bearing forces and motor torque. Nevertheless it is feasible to use two separated 3-phase systems. Concerning the heteropolar drive there is a separated 3-phases system; one for torque generation and another for force generation. The phase characteristic of both systems is shown in Fig. 5 and 6. From these phases characteristic performance factors can be derived that describe the overall behaviour of the drive in comparison to the phase characteristic [5], [7]. Due to the fact that these factors are related to the phase characteristic, they cannot be compared for different design principles, but they show that the bearingless motor operation of both reluctance motors is limited to only a few design variants. Concerning six phases only the 6-4 stator-rotor teeth design is reasonable for homopolar drives. For the six phases heteropolar flux-switching motor a bearingless operation is only feasible for the 12-10 and 12-16 topologies (when single phase torque characteristics are not under consideration).

TABLE I. GEOMETRIC AND MATERIAL PARAMETERS

Variable	Description	Value		Unit
		hom.	het.	
h_{rz}	axial rotor height	17	10	mm
d_{ro}	outer rotor diameter	65	150	mm
δ	mechanical air gap	4.8	3	mm
d_{so}	system outer diameter	130	280	mm
h_{sz}	system axial length	130	35	mm
n_r	number of rotor teeth	4	10	
n_s	number of stator teeth	6	12	
stator and rotor material		M330-50A		
stator permanent magnet material		N42	N38	

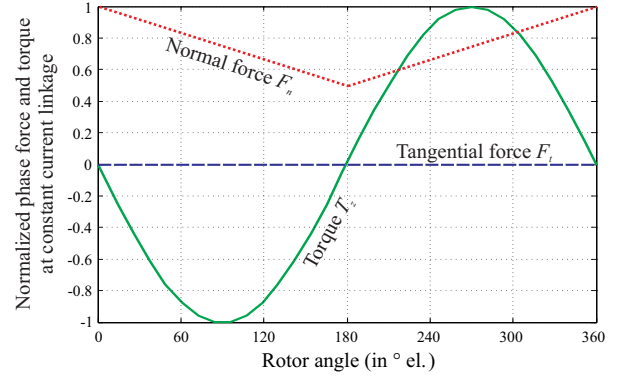


Figure 5. Resulting force and torque of one phase over the rotor angle at constant current linkage for the homopolar slice motor prototype.

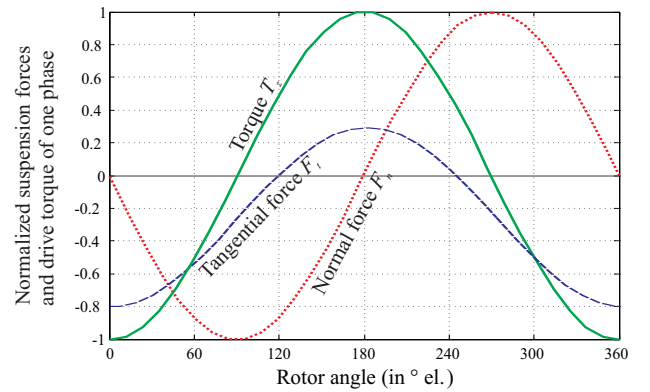


Figure 6. Bearing force (of a bearing phase) and motor torque (of a torque phase) over the rotor angle at constant current linkage for the heteropolar slice motor prototype.

However, the following analysis enables a comparison of homopolar and heteropolar torque generation capability. Assuming sinusoidal flux linkage in the coils, the drive torque

$$T(\varphi) = \frac{\partial \Psi_{PM}(\varphi)}{\partial \varphi} i_s = N_s A_{tooth} \hat{B} \cos(\varphi) \quad (2)$$

holds true. Considering non-saturated machines, for heteropolar drives the magnetic field strength in a stator tooth fluctuates in the range

$$-B_{sat} < B_{het}(\varphi) < B_{sat}. \quad (3)$$

In contrast to that, for homopolar drives the field in the tooth yields

$$0 < B_{hom}(\varphi) < B_{sat}. \quad (4)$$

Thus, it becomes clear, that for the machines of the same size with the same material utilization the homopolar and heteropolar mean drive torque can be estimated by the relation

$$\bar{T}_{het}(\varphi) \approx 2 \cdot \bar{T}_{hom}(\varphi). \quad (5)$$

This implies that for well utilized machines the torque density of homopolar drives will be superior to that of heteropolar motors. However, this consideration does not hold true for force generation. About the same force densities are possible with both machines.

C. Winding Scheme and Outline

As mentioned before the used winding schemes for the two considered drives are quite different, although both systems feature a double 3-phase star connected winding configuration. Figure 7 illustrates both of these winding systems. Due to the double 3-phase star connections only four currents needs to be measured for the nested current controllers in both prototypes.

The setting of the coil turn numbers can be considered easier in the separated winding system of the heteropolar flux-switching motor, because the suspension and drive coils can be designed independently and, thus, differently. In the combined winding system of the bearingless homopolar drive the set coil turn number influences both suspension and torque.

A remarkable issue of the two prototype drives is the poor power factor because of the large stator inductivities due to the small magnetic air gap [11].

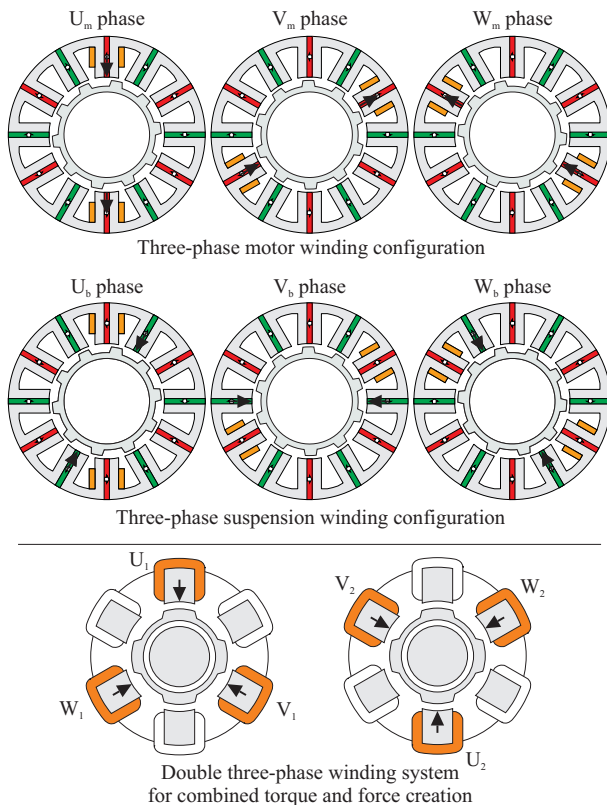


Figure 7. Winding schemes for the heteropolar (top) and the homopolar (bottom) prototype machine.

TABLE II. KEY PARAMETERS OF THE PROTOTYPEW

Variable	Description	Value		Unit
		hom.	het.	
k_r	radial stiffness	-60	-41.6	N/mm
k_z	axial stiffness	3.4	7.3	N/mm
k_ϕ	tilt stiffness	1	21.4	Nm/rad
$F_{r,p}$	force capacity/phase	20	18	mN/Aturn
$T_{r,p}$	torque capacity/phase	0.1	0.45	mNm/Aturn
N_s	windings per coil	250	80	turns
n_p	coils per phase	1	2	
n_r	rated speed	1000	3000	rpm
T_r	rated torque	0.65	1.6	Nm

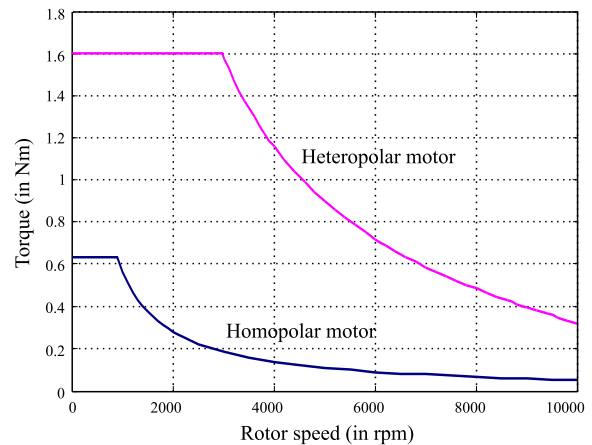


Figure 8. Torque-speed-characteristics of the two bearingless reluctance slice motors.

D. Operational Characteristic

The principal characteristics of both bearingless reluctance drives is the same as in permanent magnet excited bearingless synchronous machines. Even though the rotor has salient poles, the force and torque dependency from the stator currents is linear, due to the high permanent magnetic bias flux in the air gap. The torque created by the variance of the inductivity over the rotor angle is negligible. Force and torque measurements can be found in [6] and [7]. Figure 8 shows the torque-speed curve of both drives. It is clearly visible that the heteropolar flux-switching motor features higher output power. This is mainly because of its much larger rotor diameter and smaller air gap.

Concerning the motor losses and their efficiency measurements are currently conducted. First results are presented in [10]. Regarding the idle losses it is expected that homopolar drives are superior due to the reduced magnetic field variation.

After putting both systems into operation successfully, it can be claimed that their operational, dynamic and control characteristic and behaviour is very similar to common rotor permanent magnet excited slice motors. Thus, it has been shown that these new drive concepts represent feasible alternatives to state-of-the-art bearingless slice motors, especially in disposable systems and high temperature applications.

CONCLUSION

This paper comprises a comparison of the two bearingless reluctance slice motor prototypes. The characteristic data and main behaviour is discussed. Both drives feature a relatively low power factor due to the high inductivities of the drives. Normally, this results in a bad utilization of the power electronics. It also can be seen that the force and torque capacity per phase and ampere-turn are very similar. However, in the other characteristic parameter, like for instance the stiffnesses, high differences do exist.

The homopolar motor features reduced iron losses, a capability for higher speed and larger air gaps, but lacks of torque density. On the other hand the heteropolar motor seems not suitable for large air gaps. The high number of rotor teeth increases the electrical speed and, therefore, prohibits high mechanical speeds. The generation of force and torque capability is decoupled and can be designed independently.

Thus, the bearingless homopolar reluctance slice motor seems more suitable for applications like pumps, blowers or fans (characterized by relatively high rotational speed with low torque), whereas the bearingless heteropolar flux-switching slice motor rather works for mixers and stirrers (demanding lower speeds but higher torque).

ACKNOWLEDGEMENT

This work was supported by the Linz Centre of Competence (LCM) GmbH, a K2-centre of the COMET program of the Austrian Government. The authors thank the Austrian and Upper Austrian Government for their support.

REFERENCES

- [1] R. Schöb, N. Barletta, "Principle and application of a bearingless slice motor," *Proceedings on 5th Int. Symp. on Magnetic Bearings (ISMB)*, pp. 333-338, 1996.
- [2] T. Nussbaumer, K. Raggl, P. Boesch, J. W. Kolar, "Trends in integration for magnetically levitated pump systems," *Proceedings on Power Conversion Conf. (PCC)*, pp. 1551-1558, 2007.
- [3] B. Warberger, R. Kaelin, T. Nussbaumer, J. W. Kolar, "50Nm/2500W Bearingless Motor for High-Purity Pharmaceutical Mixing," *Proceedings on IEEE Trans. on Industrial Electronics*, vol. 59, no. 5, pp. 2236-2247, 2012.
- [4] T. Nussbaumer, P. Karutz, F. Zürcher and J. W. Kolar, "Magnetically levitated slice motors—an overview," *IEEE Transactions on Industry Applications*, vol. 47, no. 2, pp. 754-766, March-April 2011.
- [5] W. Gruber, W. Briewasser, M. Rothböck, W. Amrhein and R. Schöb, "Bearingless reluctance slice motors," *Proceedings on 13th International Symposium on Magnetic Bearings (ISMB)*, Aug. 2012.
- [6] W. Gruber, M. Rothböck, R. Schöb, "Design of a novel homopolar bearingless slice motor with reluctance rotor," *Proceedings on 5th IEEE Energy Conversion Congress and Exposition (ECCE)*, 2013.
- [7] W. Gruber, W. Bauer, K. Radman, W. Amrhein, R. Schöb, "Considerations Regarding Bearingless Flux-Switching Slice Motors," *Proceedings on 1st Brazilian Workshop on Magnetic Bearings*, Oct. 2013.
- [8] W. Gruber, K. Radman, "Design of a Bearingless Flux-Switching Slice Motor," *Proceedings on 7th Int. Power Electronics Conference, (IPEC-ECCE Asia 2014)*, May 2014.
- [9] Z. Q. Zhu, Y. Pang, J. Chen, Z. P. Xia, D. Howe, "Influence of design parameters on output torque of flux-switching permanent magnet machines," *Proceedings on IEEE Vehicle Power and Propulsion Conference (VPPC)*, pp. 1-6, 2008.
- [10] K. Radman, N. Bulic, W. Gruber, "Loss Analysis of Bearingless Flux-Switching Slice Motor," *Proceedings on 14th Int. Symp. on Magnetic Bearings (ISMB)*, accepted for publication, August 2014.
- [11] K. Radman, N. Bulic, W. Gruber, "ECCE, Performance Evaluation of a Bearingless Flux-Switching Slice Motor," *Proceedings on 6th IEEE Energy Conversion Congress and Exposition (ECCE)*, accepted for publication, Sept. 2014.